

Microstructure and mechanical properties of Fe-48(wt.%)Ni alloy processed by equal channel angular pressing

Rabeb Lachhab, Mohamed Ali Rekik, Thierry Baudin, Anne Laure Helbert, François Brisset, Mohamed Khitouni

▶ **To cite this version:**

Rabeb Lachhab, Mohamed Ali Rekik, Thierry Baudin, Anne Laure Helbert, François Brisset, et al.. Microstructure and mechanical properties of Fe-48(wt.%)Ni alloy processed by equal channel angular pressing. 2020. hal-03052337

HAL Id: hal-03052337
https://hal.science/hal-03052337

Preprint submitted on 10 Dec 2020

HAL is a multi-disciplinary open access archive for the deposit and dissemination of scientific research documents, whether they are published or not. The documents may come from teaching and research institutions in France or abroad, or from public or private research centers.

L'archive ouverte pluridisciplinaire **HAL**, est destinée au dépôt et à la diffusion de documents scientifiques de niveau recherche, publiés ou non, émanant des établissements d'enseignement et de recherche français ou étrangers, des laboratoires publics ou privés.

Microstructure and mechanical properties of Fe-48(wt.%)Ni alloy processed by equal channel angular pressing

Rabeb Lachhab[a*], Mohamed Ali Rekik[a], Thierry Baudin[b], Anne Laure Helbert[b], François Brisset[b], Mohamed Khitouni[a].

[a]*Laboratoire de Chimie Inorganique Ur-11-Es-73, Faculté des Sciences Sfax, BP 1171, 3018, Sfax Tunisie.*

[b]*ICMMO, SP2M, Univ. Paris-Sud, Univ. Paris-Saclay UMR CNRS 8182, 91405 Orsay Cedex, France.*

Abstract

The microstructure and mechanical properties of a Fe-48wt%Ni alloy in form of stacked sheets and bulk billet after severe plastic deformation using equal channel angular pressing (ECAP) were investigated. Samples were passed through a die with an inner angle of $\Phi = 90°$ and outer arc of curvature of $\psi = 17°$ at room temperature. X-ray diffraction and Electron Backscatter Diffraction were used to evaluate phase transformation and microstructure before and after ECAP process. Heterogeneous structure was identified by the formation of shear bands during severe plastic deformation. The crystallite size decreased down to 30 nm. In order to characterize the mechanical properties, tensile tests were carried out. Results of mechanical tests showed a significant loss of ductility after ECAP compared to the initial material with an increase in tensile strength from 459 MPa to a maximum value of 676 MPa. This increase is accompanied by enhanced dislocation density ($2.10^{15}m^{-2}$) and was related to grain refinement. Moreover, the alloy has shown a decrease in elongation to failure to values of approximately 22%. The fracture surface morphology shows the formation of a specific dimple relief.

Keywords: Microstructure, FeNi alloys, ECAP, EBSD, mechanical properties.

* Address correspondence to E-mail: lachhab_rabeb@hotmail.com

1. Introduction

Severe plastic deformation (SPD) has been studied extensively due to its potential to produce full density fine-grained structures with attractive physical and mechanical properties [1-5]. Among the techniques for preparing such structures, High Pressure Torsion (HPT) [6-8], Accumulative Roll Bonding (ARB) [9-13] and Equal Channel Angular Pressing (ECAP) are found [4,5,14,15]. ECAP is considered as a well-developed method to prepare materials with an ultra-fine grain (UFG) microstructure. In this process, a sample is pressed through a die having two channels of equal cross-section intersecting at an inner angle Φ and at the outer arc of curvature Ψ. During the ECAP process, although the sample undergoes severe shear deformation, it retains the same cross-sectional geometry. Therefore, the same piece can be pressed repetitively through the die channel introducing additional strain. There is much current interest in producing metals and alloys with very small grain sizes, because a reduction in grain size leads to significant material strength and toughness improvement at room temperature. The average grain size reduction during ECAP depends on several parameters including the processing route and the number of passes. So far, the main conclusions of previous investigations on the mechanical properties of metals and alloys processed by ECAP are hardening caused by grain refinement, sometimes dramatic, with a Hall–Petch-type relationship [4,5, 14,15]. Due to their low grain size, the processed samples contain, therefore, large number of grain boundaries and high amount of lattice defects, such as vacancies, dislocations, and staking faults [16,17].

Soft magnetic nickel-iron alloys containing about 30 to 80% Ni are the most ductile and most flexible alloys currently in use [18]. Their exceptional ductility permits production of thin foil or wire shapes. Furthermore, many elements can enter into solid solution, permitting tailoring of their magnetic and physical properties such as a low thermal expansion coefficient and an absence of brittleness at low temperatures, conservation properties after thermal

cycling, paramagnetic to ferromagnetic transition after polymorphism, strain hardening, etc. [18]. The nickel-iron alloys are extensively employed in various applications including electronic devices and electromagnetic shielding of computers and communication equipment.

Recently, many researchers have focused on the effect of SPD in Fe-Ni alloys. As an example, Pustov et al. [8] revealed that the temperature of $\gamma \rightarrow \alpha_2$ martensitic transformation of $Fe_{100-x}Ni_x$(x=14-28) alloys produced by mechanical alloying (MA) and HPT is reduced by 300-350K compared with conventionally prepared alloys. They attributed this decrease of temperature to small crystallite grain size (d=60-90 nm). Due to its exceptional properties, Fe-36%Ni alloy (Invar) has attracted great and unceasing attention and many studies were carried out to evaluate the texture and microstructure changes after SPD as ARB [11,12] and Cross Accumulative Roll Bonding CARB [13]. In fact, after 10 ARB cycles, elongated ultrafine grains microstructure was obtained in Fe36%Ni and according to the authors [12], six ARB cycles were enough to homogenize the UFG microstructures and the hardness of the materials without lubrication. Compared with ARB processing [12], Azzedine et al [13] have noted an improvement of Vickers microhardness up to 10% in samples processed by CARB.

As far as we know, few studies have focused on the evaluation of Fe-48%Ni alloy behavior after SPD [19-22]. Using three different approaches: Neutron diffraction, Dillamore and KAM approaches, Betanda et al [20] have measured the stored energy in severely cold rolled Fe–48%Ni sheets and they have demonstrated that the neutron diffraction method exhibits the best estimation because it takes into consideration all the dislocation types. Other study about the effect of microalloying elements sulfur and niobium on the formation of {100}<001> Cube texture in cold rolled Fe–48%Ni sheets has shown that sulfur favors and accelerates the nucleation and the development of Cube grains although niobium inhibits theses process [19]. Both prepared by ARB, Fe–48%Ni and Fe–36%Ni sheets have not

exhibited the same texture evolution and higher strength and smaller grains have been found in Fe–48%Ni [21]. In particular, the heterogeneity, in different zones of the ECAPed Fe-48%Ni material, has been studied in terms of texture and mechanical properties [22]. Shearing deformation has typically enhanced in the top and the lower zone underwent considerably less hardening.

The present work focuses on the structural, microstructural and mechanical changes occurred in Fe–48%Ni (wt.%) alloy processed by ECAP method by means of Electron BackScatter Diffraction (EBSD) and tensile tests. Microstructural of different metallurgical states is characterized in terms of crystallite size, lattice strains and dislocation density using X-ray diffraction (XRD).

2. Experimental details

2.1 Materials and experimental methods

A Fe–48%Ni (wt.%) alloy was received in the form of strips with dimensions of 300×300×1 mm^3 and 300×45×10 mm^3 and then machined into blade specimens of 1 and 10 mm thickness, 10 mm width and 60 mm length. The ECAP process was conducted at room temperature using a die with $\Phi = 90°$ and $\psi = 17°$ (Fig. 1a) using a pressing speed of 0.48 mm/s. A stacking of nine superposed samples (S.S) and a bulk billet (B.B) was introduced in the die (Fig.1b and 1c). The molybdenum disulphide (MoS_2) was used as lubricant to reduce the friction. S.S and B.B samples were ECAPed twice and once respectively. After each pass of ECAP, peripherals samples, (located in the top and in the bottom of the stack along normal direction (ND), respectively) and central sheet of S.S and three longitudinal sections with 1 mm of thickness from B.B sample were characterized. For the EBSD analysis, sections in the TD-ND plane near the center of the ECAPed sheets were prepared by mechanical polishing to a mirror-like finish and electropolishing with a Struers A2 solution at room temperature.

Microstructure analysis was carried out using a FEG-SEM Supra 55 VP scanning electron microscope operating at 20 kV. EBSD data were analyzed using the TSL Orientation Imaging Microscopy, OIM™ software. The X-ray diffraction measurements of the ECAPed Fe-Ni samples were carried out on a Siemens goniometer system with a Co-Kα radiation.

The mechanical properties of the as received and the ECAPed samples located in the middle of S.S and the central section of B.B were also evaluated at room temperature in the longitudinal direction by tensile tests. The tensile tests were carried out using a Zwick/Roell (Z010) machine with a cross head speed of 4×10^{-3} mm/s.

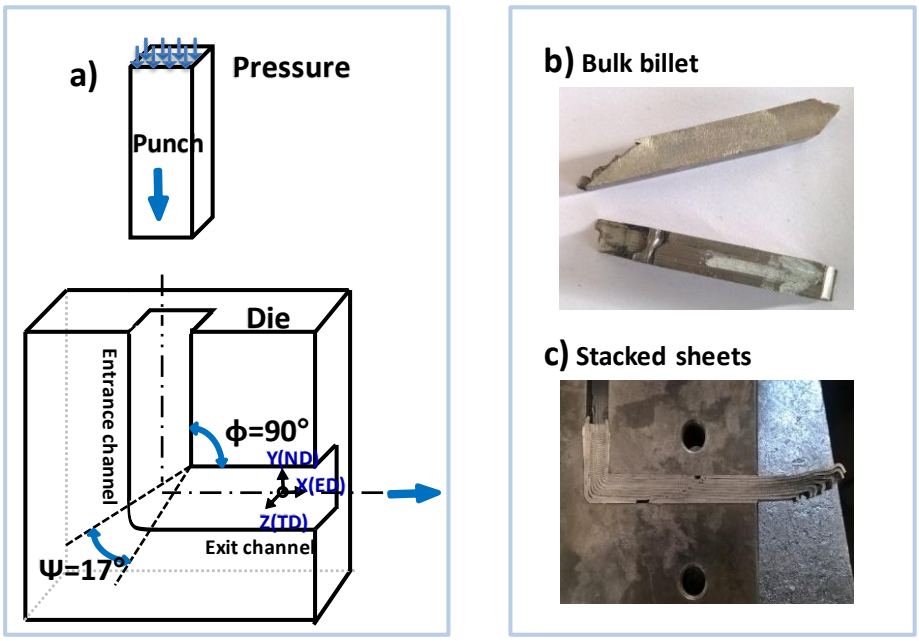


Figure 1: Schematic illustration showing the geometry of the ECAP die (a) and samples after ECAP process (b and c).

2.2 Evaluation of X-ray diffraction profiles

The a_{hkl} lattice parameter before and after ECAP was deduced from a linear regression analysis, from each peak, and plotted using the Nilson–Reley (NR) function [23].

$$NR=(\cos 2\theta/\sin\theta+\cos 2\theta/\theta)/2 \quad (1)$$

and extrapolated to NR = 0, that is $2\theta = 180°$.

The microstructural parameters such as the lattice parameter, the crystallite grain size (D), the lattice strains (ε) and the dislocation density (ρ_D) can be determined from detailed analyses of the X-ray diffraction (XRD) profiles. In the present work, the analysis of the XRD profiles was performed via the Wiliamson-Hall (WH) method widely used in numerous studies [24,25].

For severely deformed materials, dislocation density, ρ_D (m^{-2}), can be calculated in terms of the crystallite size, D, the lattice strains, ε, and the Burger's vector, b, according to formula (2) [26,27]: $\rho_D = 2\sqrt{3}\frac{<\varepsilon^2>^{1/2}}{D.b}$

Where "b" is equal to $\frac{a\sqrt{2}}{2}$ for the fcc-structure and "a" is the unit cell length.

3. Results and discussion

X-ray diffraction patterns and stress-strain curves of the as-received materials (in the form of thin and bulk sheets) showed almost the same results.

Figure 2 (a-c) illustrates the X-ray diffraction patterns of the Fe-48%Ni alloy after the ECAP process for the S.S and B.B samples. Figure 2d shows the evolution of the peak position, in different zones along ND, for all samples before and after the ECAP process.

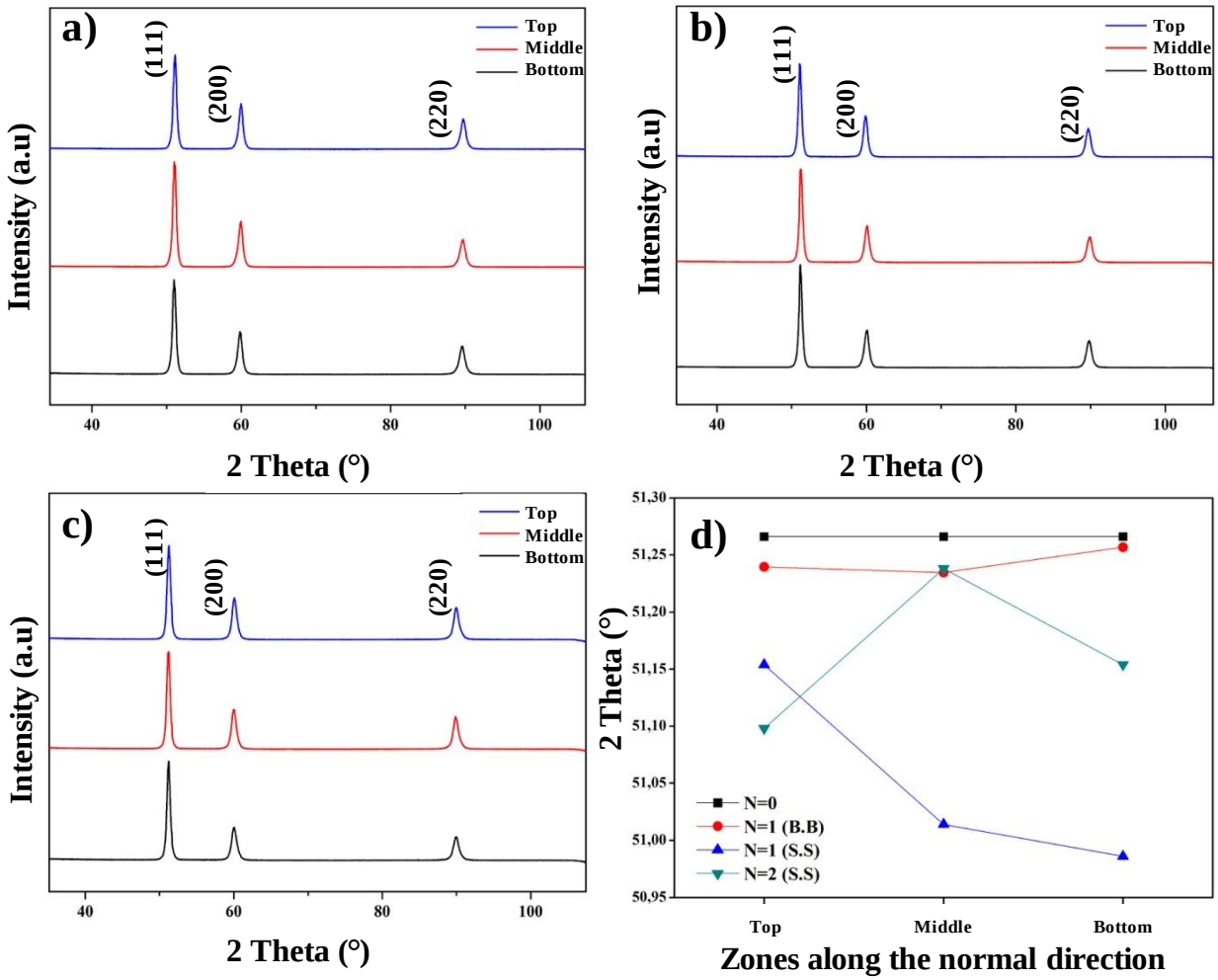


Figure 2: XRD diagrams of the Fe-48% Ni alloy after ECAP (a) 1 pass and (b) 2 passes for the stacked sheets, (c) 1 pass for the bulk billet and (d) the evolution of the (111) peak position along ND for all samples before and after the ECAP process.

The most intense peaks observed in each diffraction pattern can be indexed as the fundamental Bragg reflections (111), (200) and (220) corresponding to the γ-FeNi phase with FCC structure. By increasing the number of ECAP passes, the diffractograms do not show significant variations in the positions or shapes of different peaks. Nevertheless, the (111) peak positions in figure 2d vary slightly with the number of passes. After one pass, they are all shifted to the low values of theta. In fact, (111) peak positions in the case of S.S located at the bottom of the die are the most offset while for B.B sample, the smallest offset was in the lower zone of the die. After two passes, the (111) peaks of the S.S are shifted to higher values

of theta except for the sheets located in the upper zone of the die. Combining the Bragg law and the formula to calculate "a" in the case of a cubic structure, the following relation can be obtained:

$$a = \frac{\lambda \sqrt{h^2+k^2+l^2}}{2 \sin \theta_{hkl}} \quad (3)$$

Where h, k and l are the Miller indices, λ is the wavelength used in the XRD and θ_{hkl} is the Bragg angle.

According to formula (3), shifting in peak positions seems to depend certainly on the variation of the lattice parameter "a" resulting from a distortion in the crystal lattice. The introduction of crystalline defects in terms of dislocations and stacking defects during SPD remains the suitable explanation of this observation [27, 28].

Table 1 illustrates the evolution of the microstructural parameters in the three studied zones of (S.S) and (B.B) samples after ECAP. By increasing the number of ECAP passes, the crystallite sizes D of the different sheets decrease and the upper sheet shows the lowest value (25 nm). By comparing the results obtained for S.S and B.B after one pass, it can be noted that the crystallite size of B.B is larger than S.S particularly in the lower zone of the material.

Table 1: Microstructural parameters of Fe-48% Ni alloy after ECAP.

Passes number	**Zones along ND**	**a (Å)**	**D (nm)**	**ε (%)**	**ρ ($10^{15}m^{-2}$)**
N=1 (S.S)	Top	3.591	26.5	0.37	1.53
	Middle	3.60	27.5	0.3	1.31
	Bottom	3.602	28	0.26	1.16
	Mean value	3.597	27.33	0.31	1.33
N=2 (S.S)	Top	3.598	25	0.45	1.89
	Middle	3.583	25.5	0.45	1.81
	Bottom	3.591	27	0.35	1.38

	Mean value	3.591	25.83	0.41	1.69
N=1 (B.B)	Top	3.597	30.21	0.65	2.39
	Middle	3.596	28.56	0.58	2.26
	Bottom	3.589	32.47	0.52	1.78
	Mean value	3.594	30.41	0.58	2.14

Also, mean microstrain ε in the B.B samples (0.58%) is greater than the S.S ones (0.31%) and mainly in the higher zone of the material (0.37 and 0.65% respectively for S.S and B.B). By increasing the number of passes, the microstrain rate rises for all sheets. It should be noted that this increase is higher for the lower sheet (+35%) than for the upper one (+22%). In fact, the reduced number of passes does not favor the acquisition of a totally homogeneous microstructure [11,22], as well the effect of Φ and ψ angles and the die geometry, already mentioned by several authors [22,29-31]. Also, it is important to mention that the mean microstrain values after 2 passes remain, however, lower than those found in the B.B bulk sample ECAPed once. Even though the variation was not dramatic, the deformation of the material in the bulk state was greater than the material in the stack form. This explains the high dislocation density values (Table 1) in the case of the bulk samples ECAPed once (2.14×10^{15} m^{-2}) compared with the S.S extruded twice (1.69×10^{15} m^{-2}). This difference can be explained by the slip effect of the stacked sheets during the ECAP tests (Figure 1) which limits the homogenous distribution of strain in different sheets.

Figure 3 shows the conventional tensile curves corresponding to the initial material and the ECAPed samples. Some mechanical parameters derived from tensile tests are also given in Table 2.

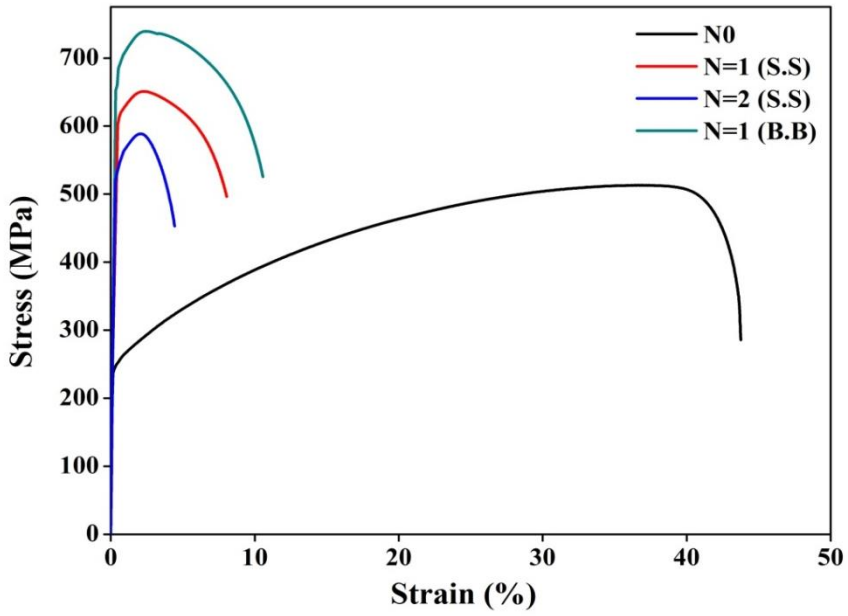


Figure 3: Stress-strain curves of Fe-48% Ni alloy before and after ECAP

It is clearly notable that the plastic domain decreases considerably after deformation by ECAP, reflecting a significant loss of ductility compared to the initial material. According to the tensile curves, the yield strength $Re_{0.2}$ increases considerably after ECAP (Table 2). Actually, as the material deforms, the grain size decreases which generates greater accumulation of dislocations at the grain boundaries. Since it requires a lot of energy to move dislocations to another grain, these dislocations accumulated along the grain boundary limit the dislocation movement and, therefore, increase the yield strength of the material [32].

Table 2: Some mechanical parameters of Fe-48% Ni alloy before and after ECAP

Samples	**Elongation to failure A (%)**	**$R_{0.2}$ (MPa)**	**R_m (MPa)**
N=0	43.7	250	512
N=1 (S.S)	8	620	651
N=2 (S.S)	4.4	450	589
N=1 (B.B)	10.5	690	739

On the other hand, the tensile strength R_m increases from 512 MPa before ECAP to 651 and 739 MPa, respectively, for S.S and B.B after one pass. The second pass reduced the value of R_m to 589 MPa.

The initial material showed an extended plastic region with a uniform deformation of about 43.7% whereas, after one pass, the elongation to failure (A) decreases to 8% and 10.5%, respectively for S.S and B.B samples. For the S.S sample, the A parameter is about 4.4% after two passes. A similar pattern of results was obtained in the Invar Fe–36wt%Ni alloy reinforced by WC nanoparticles and deformed by cold rolling [33]. In fact, the tensile strength increased by 31% and the elongation reduced from 22.7% to 4.5% after cold rolling of 25% thickness reduction. Moreover, the yield strength and tensile strength of the annealed Invar-WC are increased by 60% and 77%, respectively, compared with the Invar Fe–36wt%Ni, while after cold rolling, the values increased by 40% and 46%, respectively.

Several studies [32,34] have argued that the low elongation may be due to a limited hardening ability that promotes immediately the instability of the plastic domain and the breaking of the sample. These plastic instabilities could be favored by the presence of shear bands and microcracks after ECAP [35,36].

The following section has been an attempt to verify the formation of shear bands and microcracks within the material during ECAP. Thus, a section along [TD, ND] plane in the center of the massive material was studied by EBSD. This choice was made so as to avoid the sliding consequences noted in the case of S.S specimen. Figure 4 shows the orientation and grain boundary maps observed in B.B after its passage through the ECAP matrix.

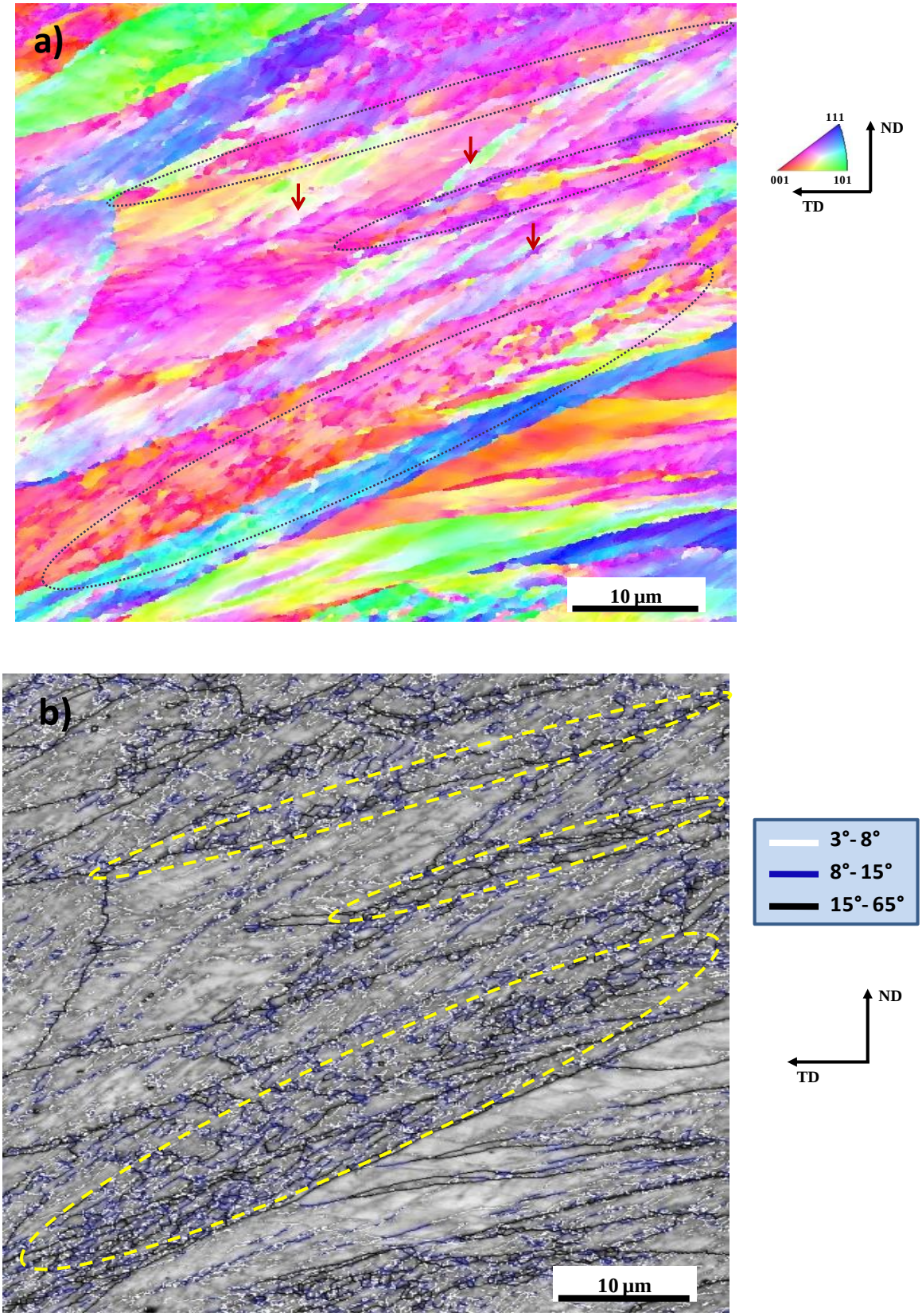


Figure 4: a) Orientations maps (IPF) ({hkl} // (TD-ND) and b) the grain boundary map in the deformed bulk billet.

In these maps, there is an alternation of quite wide bands delimited by narrow bands characterized by high concentration of dislocation walls with medium and large misorientation reflecting a localization of the plastic deformation (areas indicated by ellipses in Figures 4 a and b). Compared with existing definitions in literature, these narrow bands have the characteristics of shear bands. Another structures highlighted by red arrows (figure 4a) corresponding to small parallel bands are formed within the zones delimited by the shear bands. These bands can be considered as deformation bands.

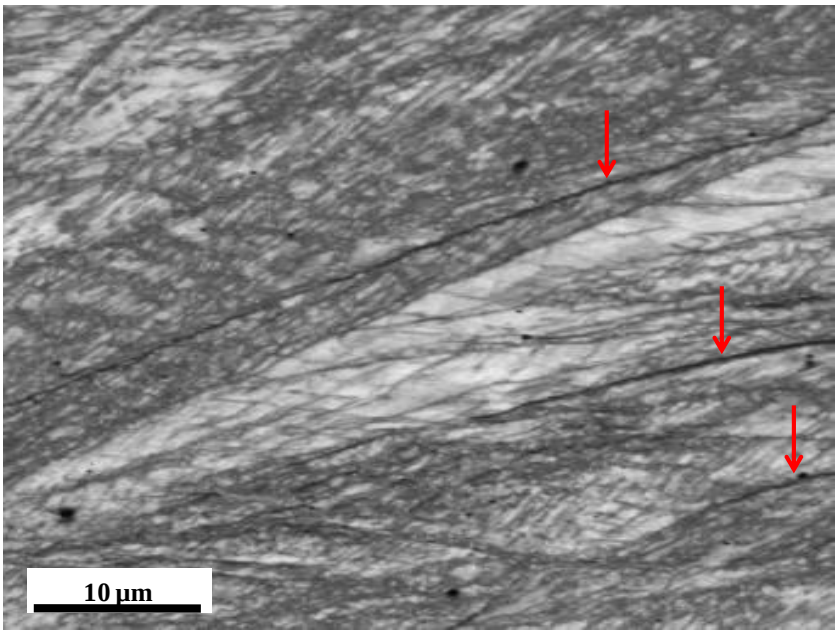


Figure 5: Image Quality map observed in the ECAPed Bulk billet.

These results go beyond older research [37], showing the formation of these two structures in pure Ni deformed by ECAP at room temperature. As it was reported in this study, the microstructure evolution during ECAP can be described in three main stages. At the beginning, the deformation starts in a homogeneous way then it becomes heterogeneous by the formation of shear bands. The transformation in the deformation type depends on several parameters including the change in the slip systems activity, the local variation in intensity of shear as well as the stress imposed by the die walls. Finally, the formation of the small deformation bands by the fragmentation of fairly homogeneous zones delimited by shear

bands. In other words, the formation of shear bands is considered as the response of the material unable to accommodate the continuation of the deformation by the formation of deformation bands. If the deformation continues, shear bands will eventually facilitate the appearance of cracks [37]. Thus, the existence of microcracks has already been demonstrated in Figure 5.

The fracture surfaces of the samples were examined by SEM after tensile tests (Figure 6). The observed surfaces are very irregular. The appearance of certain slip bands was noted especially on the surface of the specimen before ECAP. Typically, dimples appear after nucleation and coalescence of micro-voids in regions with local deformation discontinuities [38]. This confirms the material plasticity and reveals a ductile fracture type. It has been reported that the formation of large and deep dimples initiates from germination of cavities at the grain boundaries due to an accumulation of dislocations [39]. Besides, the presence of shallow dimples can be attributed to grain refinement and hardening by severe plastic deformation during ECAP as reported in the literature [40-42]. According to Lynch [41], small dimples observed on fracture surfaces indicate that cracking occurs by a localized microvoid-coalescence process along slip bands.

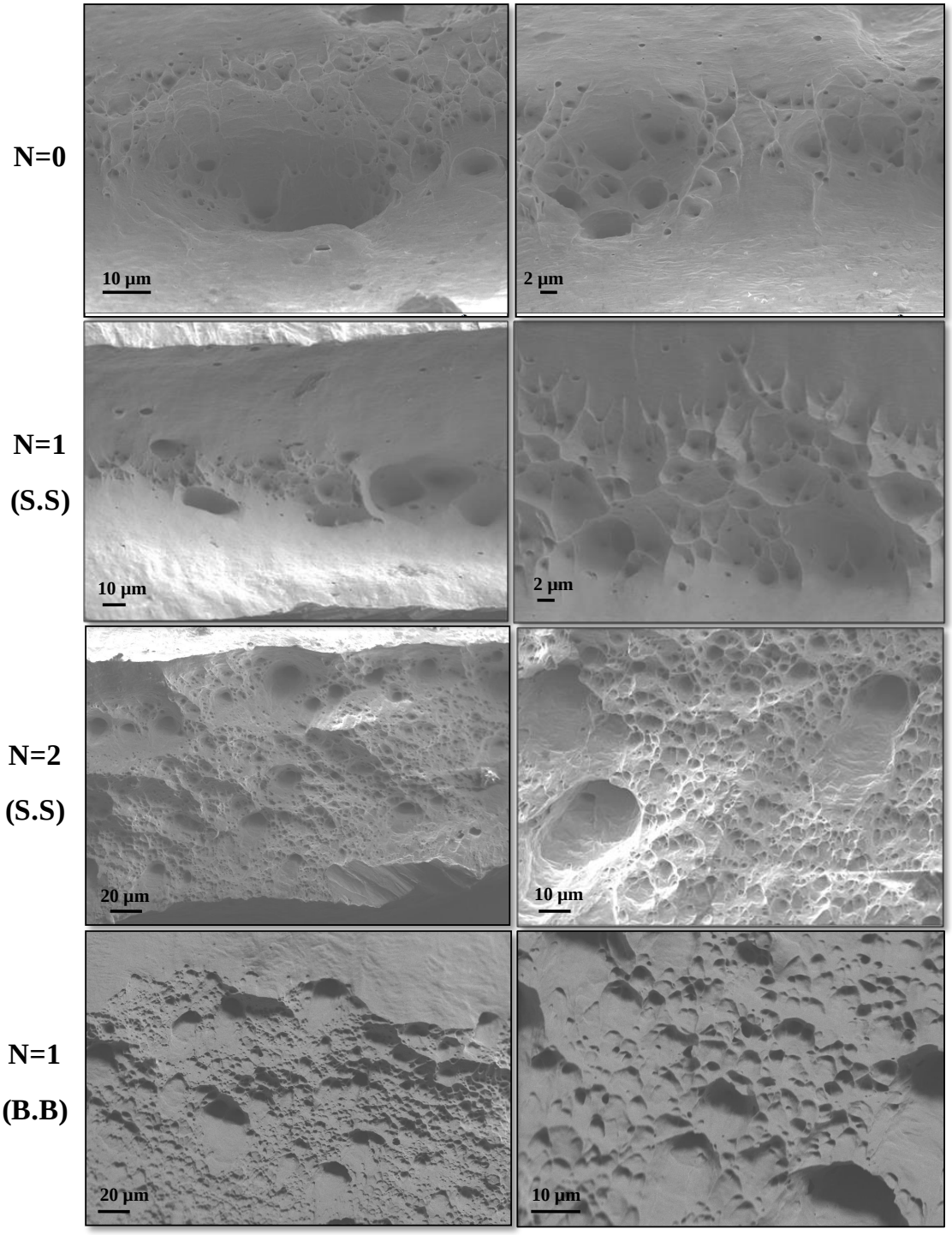


Figure 6: Fracture surfaces morphologies of the Fe-48% Ni alloy before and after ECAP.

Conclusion

A Fe-48%Ni (wt%) alloy was processed using ECAP technique at room temperature. After ECAP, the alloy provided a heterogeneous microstructure, along ND in terms of unequal distributions of microstrains rate, crystallite size and dislocation density. Generally,

the upper zones underwent the highest hardening (lowest crystallite size and largest rates of microstrains and dislocation density) compared with other ones. Particularly in the case of S.S, the sliding effect during ECAP processing offers both an irregular distribution of the deformation rate and a reduction in the hardening of the sample compared to the massive sample B.B. EBSD analyses along ED have revealed cracks and shear bands in the B.B sample after ECAP. Tensile tests have demonstrated a considerable loss of ductility. However, despite this limitation, very high yield strength and tensile strength were achieved highlighting the possibility to use the Fe-48% Ni alloy for advanced structural applications in engineering. Owing to the lack of reports about processing this alloy by ECAP, new researches are strongly needed to provide the suitable experimental conditions that respect the hardening ductility ratio.

Acknowledgements

This work was supported by the PHC-Maghreb program No. 16MAG03. Authors would like to thank R. Batonnet, Y. Ateba Betanda and T. Waeckerlé from Aperam alloys Imphy society, France, for providing the Fe–48%Ni (wt%) alloy.

References

[1] V.M. Segal, V.I. Reznikov, A.E. Drobyshevski, V.I. Kopylov, Plastic working of metals by simple shear. Russ. Metall. 1(1981)99–105.

[2] R.Z. Valiev, N.A. Krasilnikov, N.K. Tsenev, Plastic deformation of alloys with submicron-grained structure. Mater. Sci. Eng. A 137(1991)35–40.

[3] R.Z. Valiev, A.V. Korznikov, R.R. Mulyukov, Structure and properties of ultrafine-grained materials produced by severe plastic deformation. Mater SciEng A 168(1993)141–148.

[4] R.Z. Valiev, K. Islamgaliev, I.V. Alexandrov, Bulk nanostructured materials from severe plastic deformation. Prog. Mater. Sci. 45(2000)103–189

[5] R.Z. Valiev, T.G. Langdon, Principles of equal-channel angular pressing as a processing tool for grain refinement. Prog. Mater. Sci. 51(2006)881–981.

[6] R.Z. Valiev, M.J. Zehetbauer, Y. Estrin, H.W. Höppel, Y. Ivanisenko, H. Hahn, G. Wilde, H.J. Roven, X. Sauvage, T.G. Langdon, The innovation potential of bulk nanostructured materials, Adv. Eng. Mater. 9 (2007) 527–533

[7] A. Heczel, M. Kawasaki, J. L. Lábár, J. Jang, T. G. Langdon, J. Gubicza, Defect structure and hardness in nanocrystalline CoCrFeMnNi High-Entropy Alloy processed by High-Pressure Torsion, Journal of Alloys and Compounds, 711 (2017)143-154

[8] L.Y. Pustov, V.V. Tcherdyntsev, S.D. Kaloshkin, E.I. Estrin, E.V. Shelekhov, A.I. Laptev, D.V. Gunderov.Face-centered cubic phase stability and martensitic transformation under deformation in Fe–Ni and Fe–Mn alloys nanostructured by mechanical alloying and high-pressure torsion, Materials Science and Engineering A 481–482 (2008) 732–736

[9] Y.Saito, N. Tsuji, H. Utsunomiya, T. Sakai, R.G. Hong, Ultra-fine grained bulk aluminum produced by accumulative roll-bonding (ARB) process Scr Mater. 39(1998)1221-1227.

[10] A.A. Tohidi, M .Ketabchi, A. Hasannia, Nanograined Ti–Nb microalloy steel achieved by Accumulative Roll Bonding (ARB) process, Mater. Sci. Eng. A, 577(2013)43-47.

[11] F. Haj larbi, H. Azzeddine, T. Baudin, M.H. Mathon, F. Brisset, A.L. Helbert, M. Kawasaki, B. Djamel, T.G. Langdon, Neutron diffraction versus EBSD analysis of the texture in Fe-36%Ni alloy after accumulative roll bonding, J. Alloys Compd., 638 (2015)88-94.

[12] K. Tirsatine, H. Azzeddine, T. Baudin, A.L. Helbert, F. Brisset, B. Alili and D. Bradai, Texture and microstructure evolution of Fe-Ni alloy after Accumulative Roll Bonding, , J. Alloys Compd., 610 (2014) 352-360.

[13] H. Azzeddine, K. Tirsatine, T. Baudin, A. L. Helbert, F. Brisset, D. Bradai, Texture evolution of an Fe–Ni alloy sheet produced by cross accumulative roll bonding, Materials Characterization 97 (2014) 140–149

[14] T. Khelfa, M.A. Rekik, J.A. Muñoz-Bolaños, J.M. Cabrera-Marrero, M. Khitouni, Microstructure and strengthening mechanisms in an Al-Mg-Si alloy processed by equal channel angular pressing (ECAP), Int. J Adv. Manuf. Technol. 92(5-8) (2017) 1731–1740.

[15] N. Lugo, J.M. Cabrera, N. Llorca, C.J. Luis, R. Luri, J. León, I. Puertas, Grain refinement of pure copper by ECAP, Materials Science Forum 584-586 (2008)393-398.

[16] T.F. Dalla, R. Lapovok, J. Sandlin, P.F. Thomson, C.H.J. Davies, E.V. Pereloma, Microstructures and properties of copper processed by equal channel angular extrusion for 1-16 passes. Acta Mater 52(2004)4819–4832

[17] T. Ungar, A. Borbely, The effect of dislocation contrast on X-ray line broadening:A new approach to line profile analysis. J Appl. Phys. Lett. 69(1996)3173–3175.

[18] ASM Specialty Handbook: Nickel, Cobalt, and Their Alloys, Edited by J. R. Davis & Associates (2000) 92, 295

[19] Betanda YA, Helbert AL, Brisset F, Wehbi M, Mathon MH, Waeckerlé T, Baudin T (2014) Influence of sulfur on the recrystallization and {100}<001> Cube texture formation in Fe48% Ni alloys tapes. Adv Eng Mater 15:933–939

[20] Betanda YA, Helbert AL, Brisset F, Mathon MH, Waeckerlé T, Baudin T (2014) Measurement of stored energy in Fe–48%Ni alloys strongly cold-rolled using three approaches: Neutron diffraction, Dillamore and KAM approaches. Materials Science & Engineering A 614 (2014) 193–198

[21] Boudekhani-Abbas S, Tirsatine K, Azzeddine H, Alili B, Helbert A L, Brisset F, Baudin T, Bradai D (2018) Texture, microstructure and mechanical properties evolution in Fe-x (x=36 and 48 wt%) Ni alloy after accumulative roll bonding. In: IOP conference series: materials science engineering, vol 375, p 012034

[22] Rabeb Lachhab, Mohamed Ali Rekik, Hiba Azzeddine, Thierry Baudin, Anne-Laure Helbert, François Brisset, and Mohamed Khitouni. Study of the microstructure and texture

heterogeneities of Fe–48wt%Ni alloy severely deformed by equal channel angular pressing. J Mater Sci (2019) 54:4354–4365

[23] J.B. Nilson, D.P Riley, Proc. Phys. Soc. (London) 57 (1945) 160.

[24] G.K. Williamson, W.H. Hall, Acta Metall. 1 (1953) 22–31.

[25] A.I. Salimon, A.M. Korsunsky, A. NIvanov, The character of dislocation structure evolution in nanocrystalline FCC Ni-Co alloys prepared by high-energy mechanical milling, Mater. Sci. Eng. A., 271(1-2) (1999) 196-205

[26] A Vinogradov, T Ishida, K Kitagawa, VI Kopylo, Effect of strain path on structure and mechanical behavior of ultra-fine grain Cu–Cr alloy produced by equal-channel angular pressing. Acta Mater 53(2005) 2181–2192

[27] R. Lachheb, T. Bachaga, T. Makhlouf, M. Khitouni, Phase transformations and microstructural properties of nanocrystalline $Fe_{75}Si_{10}B_{10}Nb_5$ alloy synthesized by mechanical alloying, Adv. Powder Technol. 26 (2015) 1563–1569.

[28] Asma Wederni, Rabeb Lachheb, Joan Josep Suñol, Joan Saurina, Lluisa Escoda, Mohamed Khitouni, Structural, microstructural and thermal properties of nanostructured $Fe_{60}Al_{35}Sn_5$ alloy synthesized by mechanical alloying, Materials Characterization 148 (2019) 272–279

[29] T. Grosdidier, J.J. Fundenberger, D. Goran, E. Bouzy, S. Suwas, W. Skrotzki, L.S. Tóth On microstructure and texture heterogeneities in single crystals deformed by equal channel angular extrusion (2008) Scripta Mater 59 : 1087–1090.

[30] Beyerlein IJ, Tóth LS (2009) Texture evolution in equal channel angular extrusion. Prog Mater Sci 54:427–510

[31] Beyerlein IJ, Li S, Necker CT, Alexander DJ, Tomé CN (2005) Non-uniform microstructure and texture evolution during equal channel angular extrusion. Philos Mag 85:1359–1394

[32] T. Khelfa, M. A. Rekik, J. A. Muñoz-Bolaños, J. M. Cabrera-Marrero, M. Khitouni, (2018) Int J Adv Manuf Technol 95:1165–1177.

[33] Shiqi Zheng, Maximillian Sokoluk, Gongcheng Yao, Igor de Rosa, Xiaochun Li. Fe–Ni Invar alloy reinforced by WC nanoparticles with high strength and low thermal expansion. SN Applied Sciences (2019) 1:172

[34] C.C Koch, (2003) Scr Mater 49:657–662.

[35] V. Torabinejad, M. Aliofkhazraei, S. Assareh, M.H. Allahyarzadeh, A. Sabour Rouhaghdam (2017) J Alloys Compd 691: 841-859.

[36] S. Van Petegem, J. Zimmermann, H. Van Swygenhoven (2013) Acta Mater. 61 5846-5856.

[37] D. Goran, PhD Thesis, Université Paul Verlaine – Metz, LETAM, 2007.

[38] M. Meyers, K. Chawla. (2008) Mechanical Behavior of Materials. Cambridge University Press. second edition.

[39] M.A. Meyers, A. Mishra, D.J. Benson, Mechanical properties of nanocrystalline materials Progress in Materials Science 51 (2006) 427–556

[40] A. Vinogradov, T. Ishida, K. Kitagawa, V. I. Kopylo (2005) Acta Mater 53: 2181-2192.

[41] Y. G. Ko, D. H. Shin, K. T. Park, C. S. Lee (2006) Scr Mater 54: 1785-1789.

[42] D. R. Fang, Q. Q. Duan, N. Q. Zhao, J. J. Li, S. D. Wu, Z. F. Zhang (2007) Mater Sci Eng A, 459: 137-144.

[43] S.P.Lynch, Hydrogen embrittlement (HE) phenomena and mechanisms Stress Corrosion Cracking 2011, Pages 90-130